

Determination of Thermophysical Properties of Si/SiGe Superlattices with a Pump-Probe Technique

Y. Ezzahri ^(a), S. Grauby ^(a), S. Dilhaire ^(a), J. M. Rampnoux ^(a), W. Claeys ^(a).

Y. Zhang ^(b), and A. Shakouri ^(b)

(a) Centre de Physique Moléculaire Optique et Hertzienne, université Bordeaux 1,

305 cours de la libération, 33405 Talence cedex, France.

(b) Jack Baskin School of Engineering, University of California at Santa Cruz

Santa Cruz, CA 95064-1077, USA

Abstract: A Time Domain Thermo-Reflectance technique (TDTR) is used for the non-destructive evaluation of thermal and acoustic properties of Si/SiGe superlattices (SL) at room temperature. In particular, this technique allows the determination of the SL cross-plan thermal conductivity, the thermal boundary resistance at the interface between the metallic film and the SL, and the longitudinal sound velocity inside the SL. We discuss the effect of both transducer thickness and pump power on the measurements and then on values of the extracted thermophysical properties of the superlattice.

I. Introduction

The control and the stabilization of temperature are essential in microelectronics and optoelectronics, because quality and reliability of IC chips are heavily dependent on chip temperature. The temperature control of these components is typically accomplished with thermoelectric (TE) coolers. TE coolers have become essential in modern optical telecommunications to control the characteristics of laser sources, switching/routing elements, and detectors used in wavelength division multiplexed systems. Cooling requirements in microelectronic applications have also risen dramatically in recent years due to the increase in clock speed and the reduction in feature size. Generally, as these devices have become smaller, faster, and denser, the power density has greatly increased. Conventional Bi₂Te₃ TE coolers are incompatible with integrated circuits fabrication technologies, essentially silicon technology, and therefore limited in how small they can be manufactured [1]. Thus it will be very interesting if we could use silicon as efficient thermoelectric material to realize on-chip cooling solution. The existing barrier is that silicon is a very poor thermoelectric material with very low figure of merit (Z). Fortunately, recent studies [2-4] showed the possibility to enhance this parameter by introducing low dimensional structures. This has

been supported by development of epitaxial growth techniques such as molecular beam epitaxy and special kinds of chemical vapor phase epitaxy that allow the control of individual semiconductor layers on an atomic scale. This achievement provides a strong basis for designing semiconductor materials with tailored band structures and consequently tailored electronic and optical properties. The combination of different composites in the form of ultra thin layers have opened up exciting possibilities for novel devices, and it has also increased basic understanding of electronic behavior in reduced dimensions. Thermoelectricity was one of the first domains to be interested in these structures. Several measurements [5-8] have been done on different SLs in order to study their thermal and electric properties, and all agreed on the fact that these structures have a high thermoelectric power and a low thermal conductivity, compared to bulk or solid solution alloys.

Si doped Ge must receive a particular attention considering its physical properties and its very easy monolithic integration with microelectronics and optoelectronics components, this kind of SL could hence be a potential candidate to replace the conventional Bi₂Te₃ thermoelectric materials used until now. In fact SiGe has become one of the most attractive thermoelectric materials especially for high temperature applications. In this paper, we use

TDTR technique to study the thermal conductivity of two Si/SiGe superlattices at room temperature. This technique has a temporal resolution <1 ps, which is necessary to the study of fast physical phenomena, in particular thermal phenomena. Moreover, it has a nanometer-scale depth resolution [9], and therefore is well suited for measurements on very thin layers, such as SLs. More specifically, this method can isolate the effects of interface conductance from the thermal conductivity of a thin layer [10].

The main objective of our work is to determine simultaneously at room temperature, the effective cross-plan thermal conductivity of Si/SiGe SL, Kapitza resistance at the interface transducer/SL, and the longitudinal sound velocity inside the SL. Besides, we discuss the effect of the transducer thickness and the effect of the pump power on the temperature decay into the structure after absorption of the pump energy. These effects directly influence the quality of the fit, and then the value of the extracted thermophysical properties.

II. Sample description and Experimental set-up

Two samples of $1\mu\text{m}$ Si/Si_{0.7}Ge_{0.3} and Si/Si_{0.75}Ge_{0.25} SL are grown on about $500\mu\text{m}$ silicon substrate, and coated by 100nm and 12nm Al film respectively which serves as a transducer. The term “transducer” is used to specify the role of the metallic film: it converts light energy into heat which creates an acoustic wave propagating deeply in the active structure. By this way, the transducer creates the acoustic vector necessary for the analysis of the acoustic contribution in the pump-probe signal. Between the SL and the substrate is grown a $2\mu\text{m}$ buffer layer to reduce mechanical stress between both materials due to lattice mismatch between silicon and germanium which is of about 4.2% [11]. Experimental set-up is shown in figure 1. A laser beam from a 80MHz Ti: Sapphire laser with a Full Width at Half Maximum (FWHM) of 100 fs is separated into two beams with an intensity ratio of 10:1 by a nonpolarizing beam splitter. The intense pump beam is used to heat the film, while the weaker probe beam is used to monitor the reflectivity variations of the film surface which can be related to its temperature variations. The pump beam passes through an Acousto-Optic Modulator (AOM) that creates a pulse train at 574 kHz. The pump beam is focused to about $20\mu\text{m}$. The probe beam is reflected off a retroreflector mounted on a mechanical translation stage to increase the optical path length of the probe beam and hence the time delay between the pump and the probe pulses. The probe, which is centered in the heated area created by the pump pulse, is focused to about $6\mu\text{m}$ at near normal incidence. A polarizer, oriented such that only the probe beam

can cross it, is positioned before the photodiode which monitors the probe beam reflection off the sample. To improve the signal to noise ratio, the detector response at 574kHz is then monitored by a lock-in amplifier, locked on 574kHz, and analyzed by a computer.

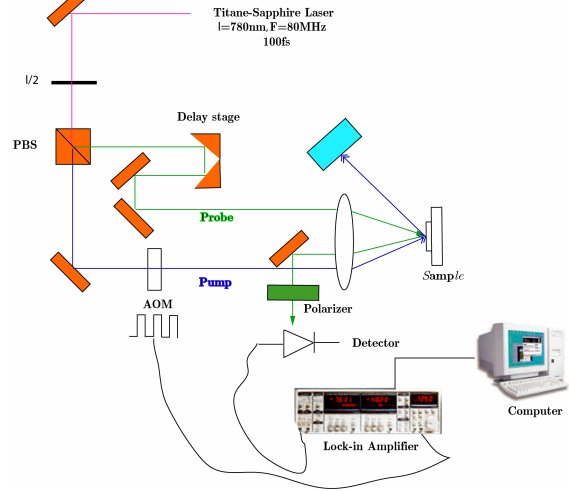


Figure 1: Experimental set up of the TDTR technique.

III. Heat transport theoretical modeling

In a TDTR technique, the determination of the thermal conductivity and interfacial thermal resistance is made by comparing the experimental cooling curve to the theoretical model and optimizing the free parameters. For all thin metal films, the temperature is homogeneous in the zone delimited by the optical penetration depth. The surface temperature variation $\Delta T_s(t)$ can be calculated using one-dimensional heat flow since the thermal diffusion length is usually much smaller than the radius of the pump beam spot. Figure 2 shows a schematic diagram (not at scale) of the studied structure with a spatial coordinate in the cross plan direction normal to the surface. Because there are two different Al film thicknesses, theoretical modeling of heat will be different from one sample to the other.

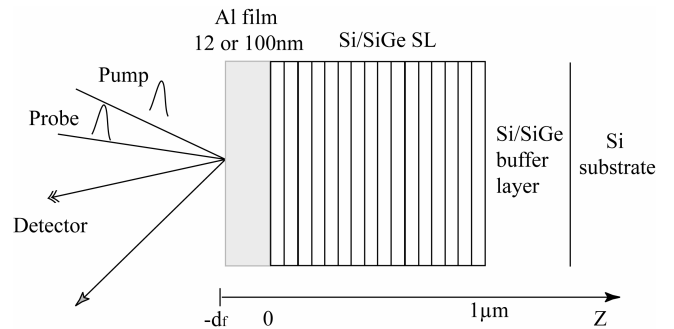


Figure 2: Schematic diagram of the whole studied structure.

1. Thin metallic film on SL

In this case, the Al film is only 12 nm thick, which is about twice the optical penetration depth $\xi=7\text{nm}$ at the wavelength of the experiment $\lambda=780\text{nm}$. After absorption of the laser pulse, all the film will be heated at the same time, and the temperature distribution will be uniform. Fourier classical heat diffusion formalism gives the following expression of the cooling of the transducer in Laplace domain:

$$\begin{aligned}\theta_f &= \frac{\tau_{sf}}{\sqrt{p\tau_{sf}}} \frac{bi + y\sqrt{p\tau_{sf}}}{bi + \sqrt{p\tau_{sf}}(bi + y\sqrt{p\tau_{sf}})} \Delta T_0 \\ &= \frac{\tau_{sf} + \tau_R \sqrt{p\tau_{sf}}}{\sqrt{p\tau_{sf}} + p(\tau_{sf} + \tau_R \sqrt{p\tau_{sf}})} \Delta T_0 \quad (1)\end{aligned}$$

where $y = \frac{(\rho c)_s}{(\rho c)_f}$, $bi = \frac{d_f}{\beta_s^\perp R_k}$, $\tau_{sf} = \frac{d_f^2}{\alpha_s^\perp y^2}$, $\tau_R = \frac{\tau_{sf} y}{bi}$

and $\Delta T_0 = \frac{(1-R)Q}{(\rho c)_f S d_f}$ where R is the reflection

coefficient of Al film, Q is the pump pulse energy, d_f is the Al film thickness, and S is the illuminated area of the Al film surface. $(\rho c)_s$, and $(\rho c)_f$ are the specific heat per unit volume of Si/SiGe SL and Al film respectively. β_s^\perp and R_k are the cross-plan thermal conductivity of the SL and Kapitza resistance at the interface Al/SL respectively.

The application of Laplace inversion theorem [12] gets a compact formula of the Al film transducer cooling in the time space:

$$\Delta T_f(t) = \frac{2\Delta T \sqrt{\tau_{sf}}}{\pi} \int_0^\infty \frac{e^{-u^2 t}}{(1 - \tau_R u^2)^2 + \tau_{sf} u^2} du \quad (2)$$

2. Thick metallic film on SL

In this case, the SL is covered by a 100 nm Al film and diffusion of heat into the transducer can not be neglected. Such as in the 12 nm Al case, theoretical modeling of heat propagation into the structure after the laser pump pulse is absorbed, is based on solving heat Fourier equations in Laplace domain. We have used Thermal Quadrupoles Method (TQM) [13], where we have done these three assumptions: (i) The characteristic time of macroscopic thermal phenomena is much greater than the laser pulse duration (about 100 fs), then the heat flux due to the laser pulse is considered to be a Dirac function of amplitude unity : $\varphi(t) = \delta(t)$, (ii) Due to the fact that the optical penetration depth in Aluminum ($\xi=7\text{nm}$) is small compared to the thickness of the film, the latter is supposed opaque, and we neglect the penetration of the light energy into it, (iii) The hypothesis of small thermal diffusivity of the SL allows us to consider the latter

as a semi-infinite medium: neither buffer-layer, nor substrate will influence the temperature variation on Al film top surface during the time scale of the experiment. After some algebra, we find this expression of the temperature variation in Laplace domain:

$$\theta_f = \frac{1}{\beta_f^\perp S q} \frac{1 + \left(1 - \frac{2}{E}\right) e^{-2qd_f}}{1 - \left(1 - \frac{2}{E}\right) e^{-2qd_f}} \quad (3),$$

where $E = 1 + \frac{\epsilon_f^\perp}{\epsilon_s^\perp} + R_k \beta_f^\perp q$, and $q = \sqrt{\frac{p}{\alpha_f^\perp}}$.

α_f^\perp , β_f^\perp , ϵ_f^\perp are respectively the cross-plan thermal diffusivity, conductivity, and effusivity of the Al film, ϵ_s^\perp is the thermal effusivity of the SL.

In the approximation of short time scale $t \rightarrow 0$, (3) can be expanded with respect to

$\Gamma = \left(1 - \frac{2}{E}\right) e^{-2qd_f}$, the inverse Laplace transform is then applied term by term, and we get these two expressions for the first order $T^{FO}(-d_f, t)$ and the second order $T^{SO}(-d_f, t)$ of this expansion respectively in the time domain:

$$\begin{aligned}T^{FO}(-d_f, t) &= \frac{1}{\beta_f^\perp S} \sqrt{\frac{\alpha_f^\perp}{\pi t}} \left(1 + 2e^{-\frac{d_f^2}{\alpha_f^\perp t}}\right) - \\ \frac{\psi \alpha_f^\perp}{2} e^{(2hd_f + \alpha_f^\perp th^2)} \text{Erfc} \left(\frac{d_f}{\sqrt{\alpha_f^\perp t}} + h\sqrt{\alpha_f^\perp t} \right) \quad (4)\end{aligned}$$

and

$$\begin{aligned}T^{SO}(-d_f, t) &= \left(\frac{2}{\beta_f^\perp S} + \frac{2\psi \alpha_f^\perp t}{R_k \beta_f^\perp} \right) \sqrt{\frac{\alpha_f^\perp}{\pi t}} e^{-\frac{4d_f^2}{\alpha_f^\perp t}} - \\ \frac{\psi \alpha_f^\perp}{R_k \beta_f^\perp} (R_k \beta_f^\perp + 4d_f + 2h\alpha_f^\perp t) \times \\ e^{(4hd_f + \alpha_f^\perp th^2)} \text{Erfc} \left(\frac{2d_f}{\sqrt{\alpha_f^\perp t}} + h\sqrt{\alpha_f^\perp t} \right) \quad (5)\end{aligned}$$

where $h = \frac{1 + \frac{\epsilon_f^\perp}{\epsilon_s^\perp}}{R_k \beta_f^\perp}$, and $\psi = \frac{8}{R_k \beta_f^\perp S}$, Erfc is the complementary error function. Then, the Al film top surface temperature variation, corrected to the second order in Γ , is given by:

$$\Delta T_f(-d_f, t) = T^{FO}(-d_f, t) + T^{SO}(-d_f, t) \quad (6).$$

We must note here that this expansion is valid for the case $\Gamma \ll 1$, which is equivalent in Laplace space to $p \gg \frac{\alpha_f^\perp}{4d_f^2}$, or $t \ll \frac{4d_f^2}{\alpha_f^\perp}$ in time space.

We have studied the sensitivity of the temperature variation on Al film top surface ΔT_f to both Kapitza resistance R_k at the interface Al film/Si/SiGe SL, and thermal diffusivity α_s^\perp of the SL, using numerical Laplace inversion [13]. This study has shown that for the 100 nm Al film, the temperature variation is more sensitive to R_k than to α_s^\perp . But for the 12 nm Al film, the cooling is more sensitive to α_s^\perp than to R_k . In the latter case, numerical calculation has shown a very small value of R_k . We can then consider a perfect thermal interface between the Al film and the Si/SiGe SL, in this case $\tau_R \rightarrow 0$, and equation (2) becomes:

$$\Delta T_f(t) = \Delta T \exp\left(\frac{t}{\tau_{sf}}\right) \text{Erfc}\left(\sqrt{\frac{t}{\tau_{sf}}}\right) \quad (7)$$

Since we measure the reflectivity change instead of the temperature variation, we must now link these two quantities, but it is well known [10] that for small temperature range, the change in reflectivity on the surface of most metals is proportional to the temperature variation:

$$\frac{\Delta R}{R}(-d_f, t) = \kappa \Delta T(-d_f, t) \quad (8)$$

where κ is the thermoreflectance coefficient.

IV. Results and discussion

Figure 3 shows the relative optical reflectivity variation on 100nm, and 12nm Al films as a function of time. We should note here that we have used normalized curves to be able to compare experimental and theoretical curves. Experimental curves depend on experimental conditions via some parameters that we cannot include in the modeling, for instance, the thermoreflectance coefficient between temperature variations and relative reflectivity variations. The absolute change in the relative reflectivity depends on the pump-power, but in our case; it was in the range 10^{-4} - 6×10^{-3} . The curves show a thermal decay on which are superimposed some spikes. These spikes arise from acoustic echoes bouncing back and forth inside the structure. The propagation of the elastic strain inside a layer alters the optical properties of this layer, in particular those of the transducer; these changes appear by consequence in the measured reflectivity signal when the elastic strain reaches the free surface and gives an echo. For the 100 nm Al curve, there is a fast thermal decay characteristic of the diffusion of heat inside the Al film, followed

by a slow decay, characteristic of the diffusion of heat inside the SL. In the opposite, the 12 nm Al curve shows only one thermal decay which describes diffusion of heat inside the SL.

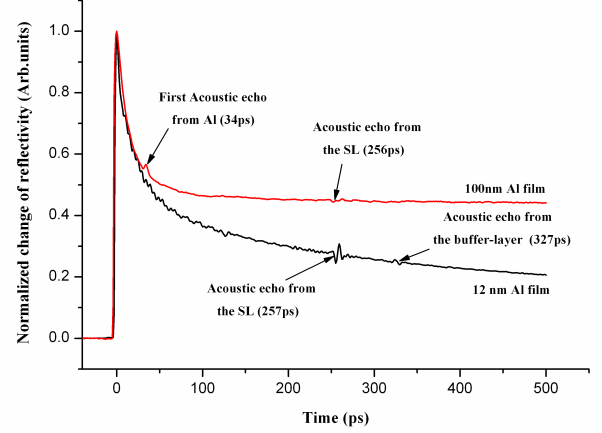


Figure 3: Experimental thermoreflectance signal of 100nm, and 12 nm Al film on Si/SiGe superlattice.

1. Thin metallic film on SL

Let us first analyze the acoustic contribution to the thermoreflectance signal. The first echo arrival time, in conjunction with the knowledge of the thickness of the Si/Si_{0.75}Ge_{0.25} SL allows us to get the sound velocity inside it we found a value $v_{Si/Si_{0.75}Ge_{0.25}} \approx 7782 \text{ m/s}$. The use of harmonic average [14] allows us to estimate the sound velocity inside Si/SiGe superlattice:

$$\frac{d_{Si/Si_{0.75}Ge_{0.25}}}{C_{Si/Si_{0.75}Ge_{0.25}}} = \frac{d_{Si}}{C_{Si}} + \frac{d_{Si_{0.75}Ge_{0.25}}}{C_{Si_{0.75}Ge_{0.25}}} \quad (9)$$

d_{Si} , $d_{Si_{0.75}Ge_{0.25}}$, $d_{Si/Si_{0.75}Ge_{0.25}}$ are respectively the thickness of Si layer, Si_{0.75}Ge_{0.25} layer and Si/Si_{0.75}Ge_{0.25} bilayer.

C_{Si} , $C_{Si_{0.75}Ge_{0.25}}$, $C_{Si/Si_{0.75}Ge_{0.25}}$ are the longitudinal elastic constants of each layer, $C_j = \rho_j v_j^2$, where ρ_j is the density, and v_j is the longitudinal sound velocity inside the layer j. $\rho_{Si/Si_{0.75}Ge_{0.25}}$ is also given by

$$\rho_{Si/Si_{0.75}Ge_{0.25}} \frac{d_{Si/Si_{0.75}Ge_{0.25}}}{d_{Si/Si_{0.75}Ge_{0.25}}} = \rho_{Si} d_{Si} + \rho_{Si_{0.75}Ge_{0.25}} d_{Si_{0.75}Ge_{0.25}} \quad (10)$$

By this way we estimate the sound velocity inside the Si/Si_{0.75}Ge_{0.25} to be $v_{Si/Si_{0.75}Ge_{0.25}} \approx 7262 \text{ m/s}$, this value is only about 7% less than the measured value.

In addition to this echo, we can also see an other echo, at $t=327\text{ps}$, which is the signature of the buffer layer.

Figure 4 shows comparison between experimental thermoreflectance signal and theoretical modeling of the 12 nm Al film case, where we have used equation (7) to fit measurements using the value of α_s^\perp obtained by Least square Method (LSM). We founded [15] $\alpha_s^\perp \approx 5 \times 10^{-6} m^2 / s$ which corresponds to $\beta_s^\perp = \alpha_s^\perp \times (\rho c)_s \approx 8.5 Wm^{-1}K^{-1}$, the specific heat c_s of the SL can be found using the same formula (10) by replacing ρ_j by c_j . The value of the cross-plan thermal conductivity found is in good agreement with that found by Huxtable et al [16] using 3ω method [17].

We should note here that the small discrepancy between theoretical curve and experimental signal can be explained by the fact that a quantity of light energy crosses the Al film and reaches directly the SL [15], which is not taken into account in the model discussed above.

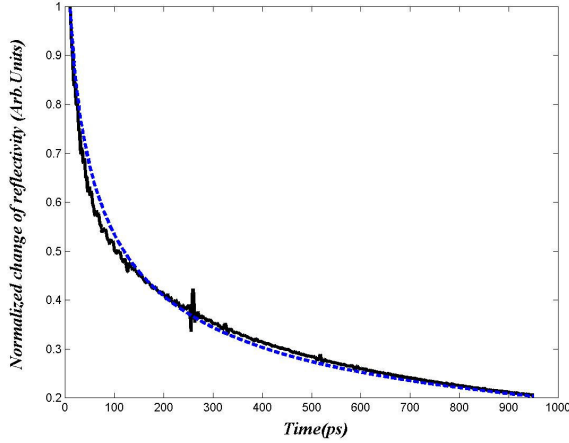


Figure 4: Comparison between experimental thermoreflectance signal (solid-line), and theoretical modeling (dashed-line) for the best fit in the case of a 12nm Al transducer, on a Si/Si_{0.75}Ge_{0.25} superlattice

2. Thick metallic film on SL

Similarly, we start analyzing the acoustic contribution. In this case, from the first echo arrival time (34 ps) and the knowledge of the bulk sound velocity in Al film ($v_{Al} \approx 6400$ m/s), we can extract the Al film thickness. We found $d_f = 108$ nm at the impact point which is in good agreement with the assumed value of 100 nm. From the second echo arrival time and the thickness of the SL, we can extract the sound velocity inside it, we find $v_{Si/Si_{0.7}Ge_{0.3}} \approx 9000$ m/s. Then we can compare this measured value to the one estimated using harmonic average [14] $v_{Si/Si_{0.7}Ge_{0.3}} \approx 7793$ m/s. In this case the estimated value is about 13% less than the measured value.

Figure 5 shows comparison between experimental thermoreflectance signal and theoretical modeling of the 100 nm Al film case, where we have used both numerical Laplace inversion transform (dashed line), and analytical inversion based on the approximation at short time scale (6) (dotted line). As we can see the two curves are quite superimposed (curves 2 and 3) at short time, and then the analytical solution diverges. This is the reason why we have used numerical inversion to fit experimental result using LSM. We see that we have a good agreement for long time greater than 100 ps. The parameters used for the best fit are: $d_f = 108$ nm, and $\alpha_f^\perp \approx 1.47 \times 10^{-4} m^2 / s$. This

implies that $\frac{4d_f^2}{\alpha_f^\perp} \approx 317$ ps and explains why the analytical solution diverges after ~ 140 ps as the validity condition ($t \ll \frac{4d_f^2}{\alpha_f^\perp}$) does not hold at this time scale.

Let us note that the value of cross-plan thermal diffusivity of Al film is very high compared to that of bulk material. In fact we should have a small one due to the small thickness of the metallic film, but this value could be understood if we take into account the low specific heat of electrons, and their large thermal penetration at the first tens picoseconds [18]. Due to the fact that the Al film surface temperature variation is more sensitive to R_k than to α_s^\perp , we have used for α_s^\perp the value obtained from the case of 12nm Al film above. Although the compositions of the two SL are different, we make the assumption that the slight difference between the SL does not cause a large difference between their thermal conductivities. Using all these parameters in conjunction with the LSM allows us to get the following value for Kapitza resistance: $R_k \approx 2.25 \times 10^{-8} m^2K/W$.

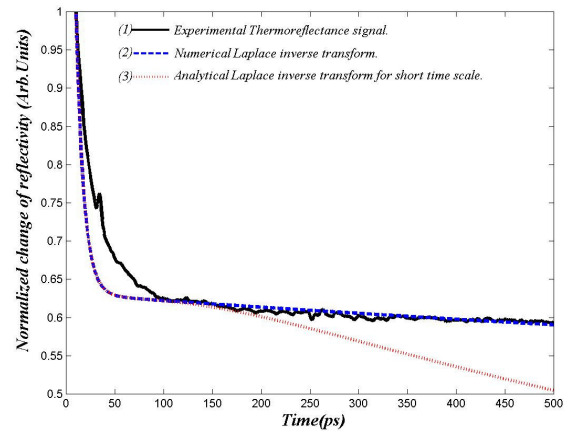


Figure 5: Comparison between experimental thermoreflectance signal and theoretical modeling for the best fit in the case of a 100nm Al transducer, on a Si/Si_{0.7}Ge_{0.3} superlattice.

This value is in reasonable agreement with that found in literature [19, 20]. We should note here that the Kapitza resistance is highly dependent on several parameters, as it was intensively discussed by R. J. Stoner and H. J. Maris [20]. It depends on: the difference of Debye temperatures between the two solids, the nature of the heat transfer process across the interface, in such a way that it can involve only phonons or both phonons and electrons, the anharmonicity of lattice potential, and the nature of the diffusion process at the interface, in such a way that it can be elastic or inelastic. In table 1, are listed all identified properties.

Properties	100nm thick transducer	12nm thick transducer
Transducer thickness (nm)	108	12
Thermal conductivity (W/m/K)	8.5*	8.5
Thermal boundary resistance ($\text{m}^2\cdot\text{K}/\text{W}$)	2.25×10^{-8}	//
SL sound velocity (m/s)	~ 9000	~ 7782

Table 1: Different properties of the two samples identified by comparison of experimental and theoretical curves, * not identified.

The discrepancy observed for the first 100ps, could be explained by the large electron thermal penetration. When the pump light is absorbed, its energy is at first communicated to electrons near the front surface of Al film which is excited to higher energy states. These hot electrons quickly diffuse away from the Al surface, but are confined to the Al film by the Schottky barrier at the interface Al/SL. Within several picoseconds, the hot electrons transfer their energy to the lattice by emission of phonons or electron-phonon collisions, slightly raising the temperature of the Al film. The depth over which electrons are able to diffuse before completely transferring their energy to phonons bath has been estimated by G. Tas and H. J. Maris to be approximately 100nm [18]. By contrast other works [21, 22] have shown that time over which the electron gas will be completely thermalized within the phonons bath is about 5ps. After this time the Al film can be characterized by one temperature which is that of the lattice. Then Fourier heat classical equation can properly be applied.

Another assumption to explain the discrepancy is the effect of the pump power. In fact, in the majority of the models used in TDTR to extract thermophysical properties, we assume that the

properties of the structure are temperature independent. The high value of the pump peak power (about 10 kW) in conjunction with the slow cycle rate due to the modulation of the pump beam could modify the film properties via an increase of its temperature. To check this effect, we have done some measurements on the same structure following the same experimental process and varying the pump power. The results are shown in figure 6.

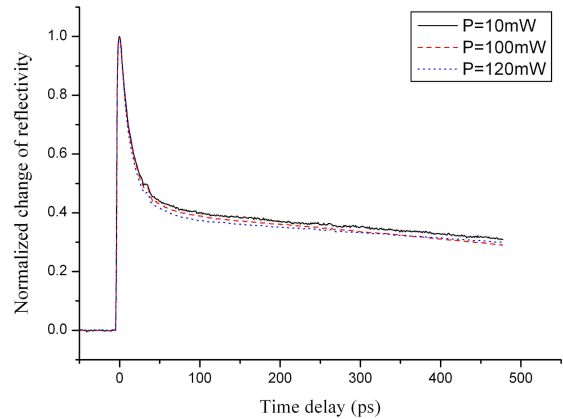


Figure 6: Experimental thermoreflectance signal of 100nm Al film on Si/SiGe superlattice with different pump powers.

As we can see, the influence of the pump power does not seem significant as the thermal decay does not vary much. We are making new experiments to be sure that the thermal decay does not depend on pump power.

We are now working to make more experimental measurements to explain the discrepancy on the first 100ps and to develop an accurate modeling of the energy transport in thick metallic film at short time scale which must include microscopic interactions between electrons themselves and between the phonons bath, as well as the temperature dependence of the physical properties. In this case, a possibility to access absolute temperature measurement on the sample will be more difficult since the relation between reflectivity change and temperature change will be more complicated.

V. Conclusion

In this paper, two Si/SiGe superlattices structure, with slight different compositions, covered by different thickness Al transducers were studied using TDTR technique. Taken into account the short time scale of the experiment, we have shown the influence of the transducer thickness on the sensitivity of the measurement to the thermophysical properties of the underlying superlattices. By this way we were able to measure both cross-plan thermal conductivity of the SL and

the Kapitza resistance at the interface transducer/SL. We were also able to estimate the sound velocity inside the Si/SiGe SL from the arrival time of acoustic echoes. This technique therefore proved to be a useful tool to characterize both thermophysical and mechanical properties of thin film multilayers. The preliminary results show that the discrepancy between experimental and theoretical curves observed in the case of thicker transducer, could not be explained by the effect of the pump power. Diffusion of electrons and then the penetration of the heat source seems to be responsible for this behavior. A more precise model which takes into account this effect should be the convenient solution.

VI. References

- [1] C. Labounty, A. Shakouri, and J. E. Bowers, "Design and Characterization of thin film microcoolers", *J. Appl. Phys.* **89**, 4059-4064, 2001.
- [2]: L.D. Hicks, and M. S. Dresselhaus, "Effect of quantum-well structures on the thermoelectric figure of merit", *Phys. Rev. B*, **47**, 12727-12731, 1993.
- [3]: J. O. Sofo, and G. D. Mahan, "Thermoelectric figure of merit of superlattices", *Appl. Phys. Lett.* **65**, 2690-2692, 1994.
- [4]: D. A. Broido, and T. L. Reinecke, "Effect of superlattice structure on the thermoelectric figure of merit", *Phys. Rev. B*, **51**, 13797-13800, 1995.
- [5] S. M. Lee, D. G. Cahill, and R. Venkatasubramanian, "Thermal conductivity of Si-Ge superlattices", *Appl. Phys. Lett.* **70**, 2957-2959, 1997.
- [6] B. Yang, W. L. Liu, J. L. Liu, K. L. Wang, and G. Chen, "Measurements of anisotropic thermoelectric properties in superlattices", *Appl. Phys. Lett.* **81**, 3588-3590, 2002.
- [7] S. T. Huxtable, A. R. Abramson, T. Chang-Lin, A. Majumdar, C. LaBounty, X. Fan, G. Zeng, J. E. Bowers, A. Shakouri, and E. T. Croke, "Thermal conductivity of Si/SiGe and SiGe/SiGe superlattices", *Appl. Phys. Lett.* **80**, 1737-1739, 2002.
- [8] M. N. Touzelbaev, P. Zhou, R. Venkatasubramanian, and K. E. Goodson, "Thermal characterization of Bi₂Te₃ /Sb₂Te₃ superlattices", *J. Appl. Phys.* **90**, 763-767, 2001.
- [9] D. G. Cahill, W. K. Ford, K. E. Goodson, G. D. Mahan, A. Majumdar, H. J. Maris, R. Merlin, S. R. Phillpot, "Nanoscale thermal transport", *J. Appl. Phys.* **93**, 793-818, 2003.
- [10] W. S. Capinsky, H. J. Maris, T. Ruf, M. Cardona, K. Ploog, and D. S. Katzer, "Thermal-conductivity measurements of GaAs/AlAs superlattices using a picosecond optical pump-and-probe technique", *Phys. Rev. B*, **59**, 8105-8113, 1999.
- [11] J. P. Douglas, "Si/SiGe heterostructures: from material and physics to devices and circuits", *Semicond. Sci. Technol.* **19**, 75-108, 2004.
- [12] H. S. Carslaw, and J. C. Jaeger, "Conduction of Heat in Solids", Oxford University Press, second edition, p302, 1959.
- [13] D. Maillat, S. André, J. C. Batsale, A. Degiovanni, and C. Moyne, "Thermal Quadripoles: Solving of Heat Equation through Integral Transforms", Wiley edition, p342, 2002.
- [14] C. Rossignol, B. Perrin, B. Bonello, P. Djemia, P. Moch, and H. Hurdequint, "Elastic properties of ultrathin permalloy/alumina multilayer films using picosecond ultrasonics and Brillouin light scattering", *Phys. Rev. B*, **70**, 94102-94113, 2004.
- [15] Y. Ezzahri, S. Dilhaire, S. Grauby, J. M. Rampnoux, W. Claeys, Y. Zhang, G. Zeng, and A. Shakouri, "Study of Thermomechanical Properties of Si/SiGe Superlattices using Femtosecond Transient Thermoreflectance Technique", Accepted in *Applied Physics Letters*.
- [16] S. T. Huxtable, A. R. Abramson, A. Majumdar, A. Shakouri, and E. T. Croke, "The effect of defects and acoustic impedance mismatch on heat conduction SiGe based superlattices", International Mechanical Engineering Congress and Exhibition (IMECE 2002), New Orleans, LA, Nov, 1-5, 2002.
- [17] D. G. Cahill, *Rev.Sci.Instrum.*, "Thermal conductivity measurement from 30 to 750K: the 3 ω method", **61**, 802-808, 1990.
- [18] G. Tas, and H. J. Maris, "Electron diffusion in metals studied by picosecond ultrasonics", *Phys. Rev. B*, **49**, 15046-15054, 1994.
- [19] A. N. Smith, J. L. Hostetler and P. M. Norris, *Microscale Thermophysical Engineering*, "Measurement of Thermal Boundary Resistance between Thin Metal Films and Dielectric Substrates", **4**, 51-60, 2000.
- [20] R. J. Stoner, H. J. Maris, "Kapitza conductance and heat flow between solids at temperatures from 50 to 300K", *Phys. Rev. B*, **48**, 16373-16387, 1993.
- [21] T. Q. Qiu, C L. Tien, "Short-Pulse laser heating on metals", *J. Heat Transfer*, **35**, 719-726, 1992.
- [22] T. Q. Qiu, C L. Tien, "Heat Transfer Mechanisms During Short-Pulse Laser Heating of Metals", *J. Heat Transfer*, **115**, 835-841, 1993.